

Supplementary Material

S1. Parameter sensitivity analysis

As formulated in Section 2, SARM has only adjustable parameters, f_a and n_{min} . We use the nine daily VIIRS-SNPP scenes shown in Fig. 7, and the corresponding nine VIIRS-NOAA-20 daily scenes to conduct a sensitivity analysis with respect to these adjustable parameters. We use three values for parameter $f_a = 0.70, 0.90,$ and 0.95 , and three values for the parameter $n_{min} = 6, 10,$ and 14 . The SARM imagery derived with the nine different combinations of these parameter values are shown in Fig. S1. Overall, the results are not very sensitive to variations of f_a and n_{min} . In general, choosing smaller values of f_a and n_{min} can lead to more cloud shadow contamination, which is slightly apparent in Fig. S1a, while larger values of these parameters may increase cloud contamination. The RMSD values, calculated for SARM imagery obtained with various combinations of parameters f_a and n_{min} , are summarized in Table S1. The left part of Table S1 shows variation of RMSD with respect to the reference image in Fig. 8d, whereas the right part of Table S1 shows the variation of RMSD with respect to the SARM results in Fig. 8c. The changes in RMSD with respect to the reference image are quite small, confirmed by barely noticeable variation in images in Fig. S1. The RMSD values with respect to the SARM results obtained with the nominal values of parameters are generally smaller than those with respect to the reference image.

Table S1. RMSD of SARM results with variation of f_a and n_{min} with respect to the reference image (Fig. 8d), and with respect to the SARM results in Fig. 8c obtained with the nominal values of parameters ($f_a = 0.90; n_{min} = 10$). The units of RMSD are the same as the digital numbers corresponding to the 8-bit color channels, ranging from 0 to 255.

| n_{min} | RMSD vs. Reference image | | | | RMSD vs. SARM ($f_a = 0.90; n_{min} = 10$) | |
|-----------|--------------------------|--------------|--------------|--------------|---|--------------|
| | $f_a = 0.70$ | $f_a = 0.70$ | $f_a = 0.90$ | $f_a = 0.95$ | $f_a = 0.90$ | $f_a = 0.95$ |
| 6 | 10.3 | 10.3 | 10.0 | 5.4 | 1.1 | 6.4 |
| 10 | 9.7 | 9.7 | 10.0 | 3.5 | 0.0 | 4.0 |
| 12 | 10.6 | 10.6 | 10.8 | 3.4 | 3.1 | 3.5 |



Figure S1. SARM imagery obtained with different combinations of the adjustable parameters (f_a , n_{min}) of (a) (0.70, 6), (b) (0.90, 6), (c) (0.95, 6), (d) (0.70, 10), (e) (0.90, 10), (f) (0.95, 10), (g) (0.70, 14), (h) (0.90, 14), and (i) (0.95, 14). Panel (e) is obtained with the nominal values of parameters (0.90, 10) and same as in Fig. 8c.

S2. Application to geostationary satellite sensor imagery

The Geostationary Ocean Color Imager (GOCI) onboard the Korean Communication, Ocean and Meteorological Satellite (COMS) provides the reflectance data and imagery in eight spectral bands with a spatial resolution of about 500 m up over the East Asian region, producing up to eight hourly snapshots per day and regional ocean color products. In Fig. S2, we show that daily clear sky imagery can be derived with SARM (Fig. S2i) from the GOCI hourly imagery (Fig. S2a–h). We note that while most of the fast-moving clouds are removed in the SARM imagery, some cloud remnants may remain, given the relatively small number of eight hourly sample images. The number of minimum samples used by the SARM was chosen as $n_{min} = 4$ for this case. We note

that other geostationary sensors may be able to capture more frequent imagery snapshots, however, that still may not help with removing large slow-moving clouds.

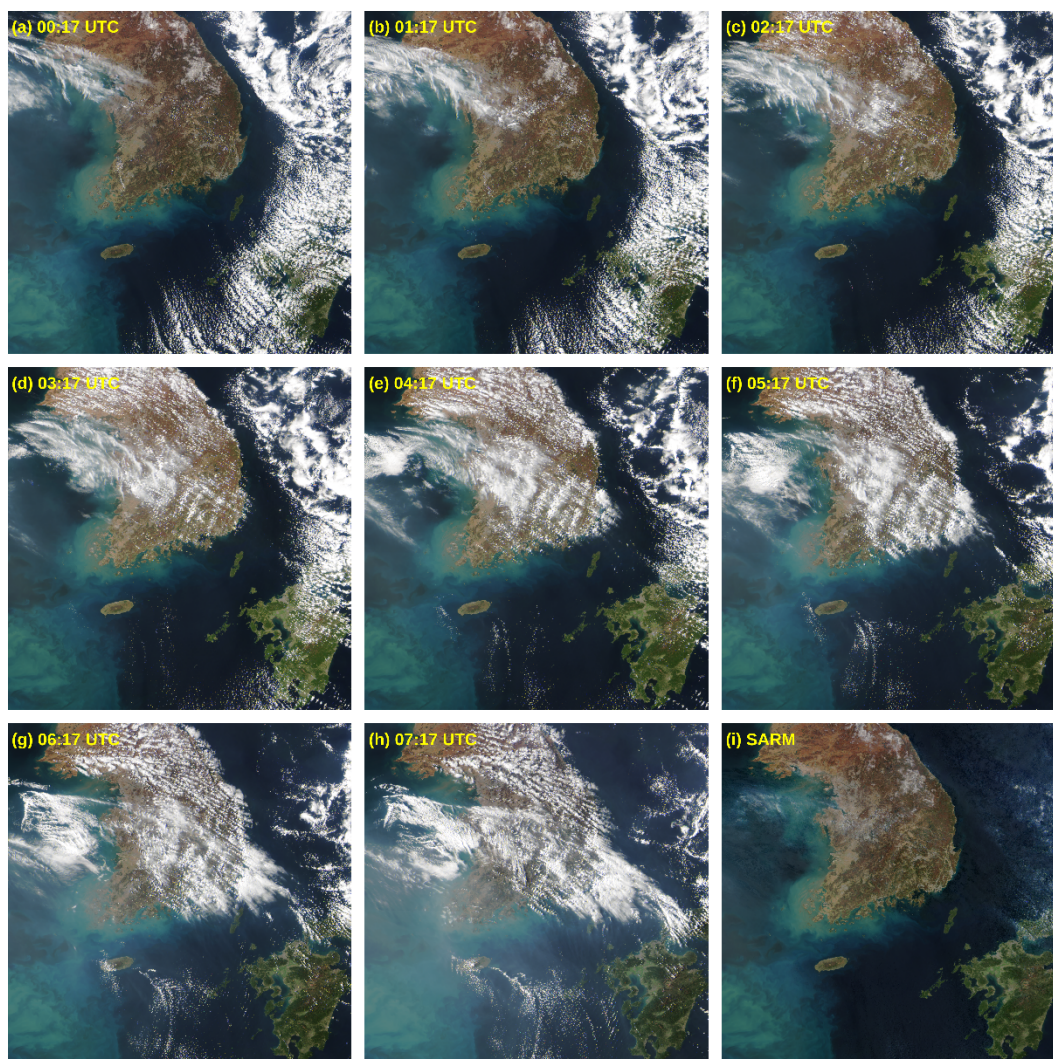


Figure S2. Examples of imagery from the geostationary ocean color GOCI sensor over the South Korean Ppeninsula and Japanese Kyushu Island (lower right) on April 1, 2019, acquired hourly at (a–h) 00:17 to 07:17 UTC (eight images), compared with (i) the SARM-derived imagery from these hourly images.

S3. Application to high resolution Sentinel-2 MSI imagery

In order to compare and to highlight the differences with other image restoration methods, we show an application of SARM to a large-scale Sentinel-2 MSI imagery for the example presented by Zhang et al. (2020). Four partially cloudy Sentinel-2A MSI scenes from August – September 2018 over Bratislava, Slovakia (Fig. S3a–d) are used to derive the clear sky imagery. The SARM results derived without the help of cloud mask (Fig. S3e) show significant cloud shadow

contamination. However, if the clouds and cloud shadows are masked out in the original daily imagery before SARM is applied, then the resultant clear sky imagery (Fig. S3f) is significantly improved. At the same time, using the cloud mask introduces some gaps in SARM results (Fig. S3f), which can be filled by using the imagery from SARM results in Fig. S3e. The composite image (Fig. S3g) thus has a complete coverage with few cloud and cloud shadow artifacts, and can be compared with the reference daily imagery from September 10, 2018, in Fig. S3h, which was not used to derive the SARM results. Imagery of the regions highlighted in Fig. S3e–h by the orange boxes is shown in detail in Fig. S4, further confirming that using the cloud mask significantly improves SARM results.

Overall, in comparison with the recent spatio-temporal image reconstruction methods, SARM is not designed for a very small number of scenes, and cannot recover the temporal evolution. However, if a reliable cloud mask is used, SARM can still produce representative results that are comparable to those obtained with other recently developed methods. Alternatively, the lack of need for the cloud mask by SARM generally can be seen as advantageous in cases where only true or false color imagery is available. In addition, relative computational simplicity of the SARM is another advantage for large-scale routine clear-sky imagery production, especially compared with machine learning techniques which require large training data sets and lengthy training times.

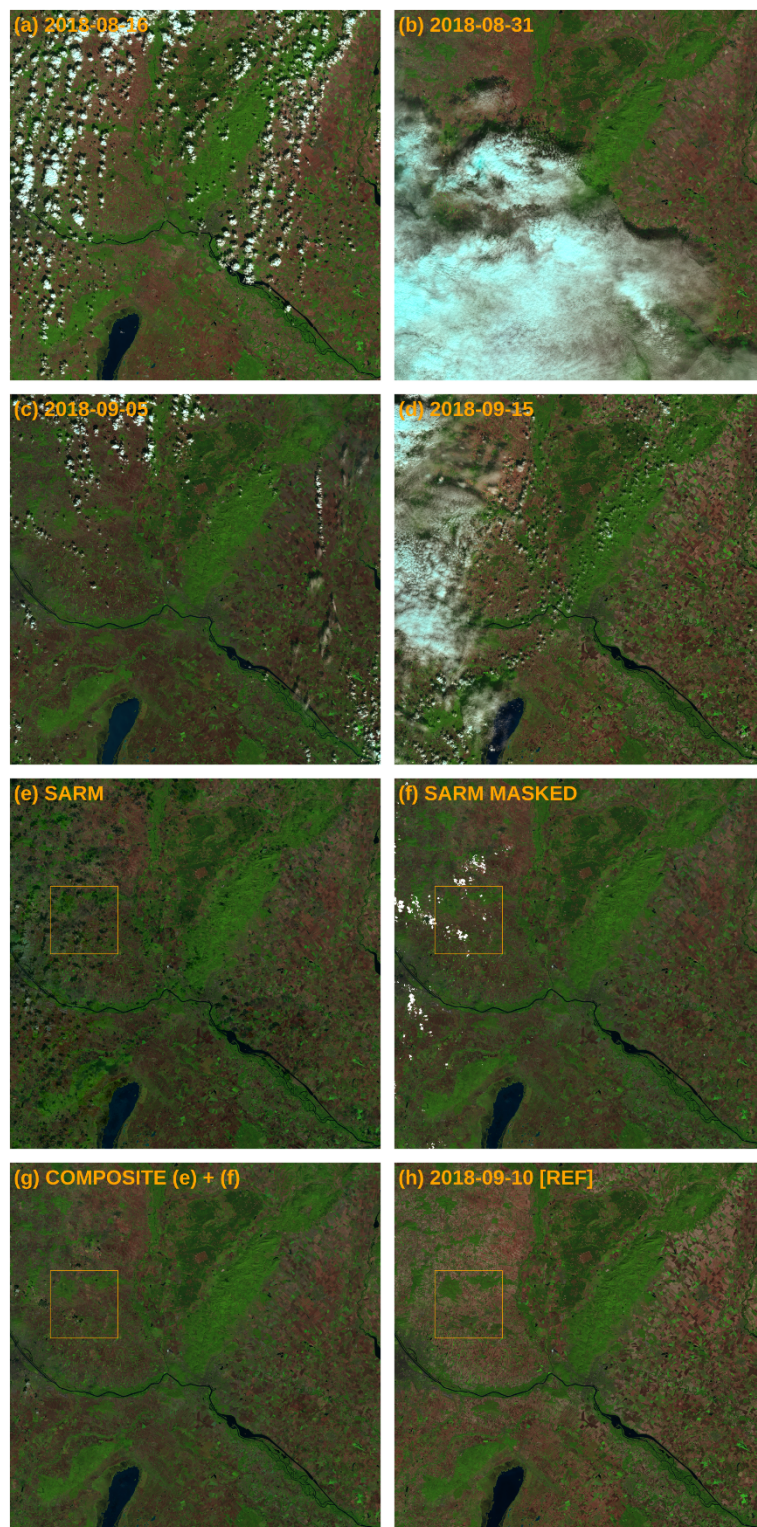


Figure S3. Examples of Sentinel-2 MSI daily imagery over Bratislava, Slovakia for (a) August 16, 2018, (b) August 31, 2018, (c) September 5, 2018, and (d) September 15, 2018. The SARM results without the use of cloud mask are shown in panel (e), and with cloud mask applied in panel (f). The composite of (e) and (f) in panel (g) shows minimal cloud or cloud shadow

effects, and is comparable to clear sky daily imagery from September 10, 2018 (panel h). Regions highlighted by orange boxes in panels (e–h) are shown in detail in Fig. S4. Sentinel-2 bands B05, B07, and B11 are used for the red, green, and blue channels, respectively, for this false color imagery.

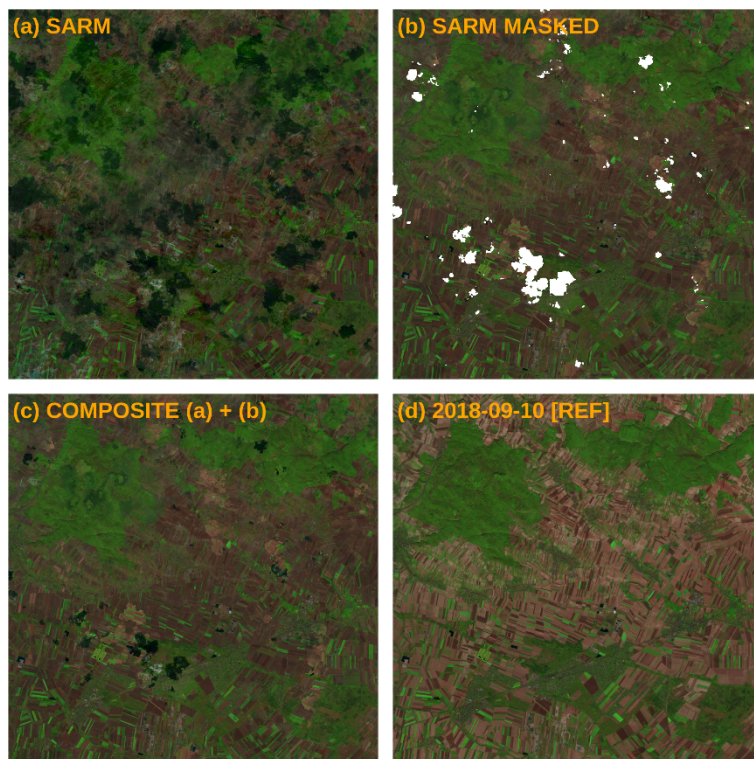


Figure S4. Detail of imagery highlighted by orange boxes in Fig. S3e–h for (a) the SARM results without the use of cloud mask, (b) the SARM results with cloud mask applied, (c) the composite of (a) and (b) showing less cloud or cloud shadow effects, and (d) comparable with clear sky daily reference imagery from September 10, 2018.